# Performance Analysis of Decision Feedback and Linear Equalization schemes for Non-Directed Indoor Optical Wireless Systems

Georgia Ntogari
Department of Informatics and Telecommunications, University of Athens, Greece
Email: gntogari@di.uoa.gr

Thomas Kamalakis and Thomas Sphicopoulos
Department of Informatics and Telecommunications, University of Athens, Greece
Email: {thkam, thomas}@di.uoa.gr

***Abstract*— Indoor optical wireless systems provide an attractive alternative for realizing next generation Wireless Local Area Networks (WLANs). In this paper, the potential of non-directed, equalized optical wireless systems is theoretically investigated, taking into account the indoor channel impulse response and the characteristics of ambient light noise and thermal noise at the receiver. Three modulation schemes, Pulse-Position-Modulation, On-Off Keying and Pulse Amplitude Modulation, are combined with appropriate equalization methods in order to mitigate the effect of intersymbol interference induced by the infrared chanel. It is shown that the various non-directed configurations can provide data rates of the order of 100Mb/s and beyond, over a medium sized room.**

***Index Terms*—wireless infrared communications, decision feedback equalization, linear equalization, pulse position modulation (PPM), on-off keying (OOK), pulse amplitude modulation (PAM)**

## I. INTRODUCTION

As the demand for ultra broadband wireless access home networks constantly increases, the radio frequency spectrum is becoming extremely congested and thus, attention is drawn towards alternative technologies. Indoor infrared wireless communications were first proposed by Gfeller and Bapst [1] and are since attracting growing interest due to the abundance of unregulated bandwidth, which renders them an attractive candidate for high speed data communications. In addition, the short carrier wavelength and large square-law detector, used in such systems, provide an inherent spatial diversity that prevents multipath fading [2]. Furthermore, as the infrared radiation does not penetrate walls, it makes it easier to construct cell-based secure networks by reusing the same wavelength in different rooms of an office building. Thus, infrared wireless Local Area Networks (LANs) can potentially achieve a very high aggregate capacity.

The infrared channel is not without drawbacks, however. In many indoor environments, it is not easy to achieve a high Signal-to-Noise (SNR) ratio, since there may be intense ambient infrared noise [3]. This noise is due to the infrared spectrum components arising from the radiation of tungsten or fluorescent lamps and sunlight. In addition, artificial light introduces significant in-band components for systems operating at bit rates up to several Mb/s and thus induces interference [4], [5]. Moreover, the power constraints on infrared transmitters imposed by eye-safety regulations, may limit the range of these systems. Infrared links are also susceptible to shadowing caused by objects or people positioned between the transmitter and the receiver.

The effect of blocking can be dealt with, by using non-directed configurations, in which the optical link does not rely on the Line Of Sight (LOS) path between the transmitter and the receiver. Compared to LOS systems, non directed configurations suffer from higher path loss imposing the need for higher levels of transmitted power and larger photodetecting area at the receiver. The multipath propagation observed, gives rise to intersymbol interference (ISI), which becomes critical at high data rates. Nevertheless, to date, the non-directed configurations, have received great interest from the research community, and a number of experimental links has been reported covering bit rates up to 50 Mb/s [6].

The objective of this work is to examine the performance of non directed indoor infrared wireless systems assuming different transmitter and receiver configurations like the ones in [7]. In the first configuration, classified as vertically oriented, the main lobe of the transmitter and the receiver is directed upwards, towards the ceiling. In the second one, classified as horizontally oriented, some of the lobes are also directed parallel to the ceiling, potentially offering a LOS path and possibly higher coverage.

The performance of these two systems is evaluated in terms of the electrical SNR, taking into account the ISI arising from multipath propagation and ambient light noise. Accurate models for the ambient light noise power distribution as well as for the diffuse infrared channel impulse response of both configurations were employed. These models were developed by the authors using MATLAB software. In previous work [8] the authors examined the performance of one-level modulation schemes with different equalization schemes, such as Maximum-Likelihood-Sequence-Estimation (MLSE),

Manuscript received April 1, 2009; revised June 20, 2009; accepted June 30, 2009.


doi:10.4304/jcm.4.8.565-571

Linear Mean-Square-Error Equalizer (LE-MSE) and Decision-Feedback Equalizer (DFE). In this work a multi level Pulse Amplitude Modulation (PAM) scheme is also considered and compared to Pulse Position Modulation (PPM) and On/Off Keying (OOK). It is shown that non-directed systems may support data rates of 100Mb/s and beyond (Fast Ethernet), making a suitable candidate for future home and office wireless LANs.

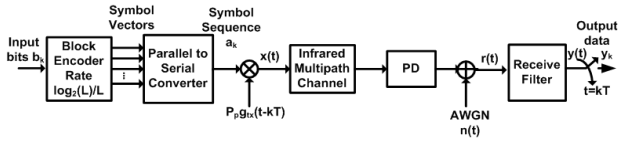


Figure 1.The indoor optical wireless system model.

## II. INDOOR INFRARED SYSTEM MODEL

The indoor infrared system model used in this paper is shown in Figure 1. In indoor infrared links, intensity modulation with direct detection is employed, where the intensity of the optical carrier is modulated by the data to be transmitted. The choice of the modulation scheme may significantly affect the performance of the system. OOK provides bandwidth efficiency at the expense of high optical power [9] whereas PPM offers an improvement in power efficiency at the cost of a poorer bandwidth. Both schemes rely on the use of two power levels to transmit data and have high peak to average power ratios. However, the price paid is their inefficient use of the available bandwidth. Thus, multilevel modulation schemes, i.e. PAM, become an attractive candidate for wireless applications as they offer improvement in bandwidth efficiency by transmitting more information per symbol. Nevertheless, multilevel modulation methods are more sensitive to non-linearities and noise.

The power, $x(t)$, of the transmitted signal is:

$$x(t) = P_p \sum_k a_k g_{tx}(t - kT) \tag{1}$$

where $g_{tx}(t)$ is the transmitter pulse shape, $P_p$ the peak power, $a_k$ are the transmitted symbols according to the level L of the selected modulation scheme ($L$=2 for OOK and $L$=4 for 4-PPM and 4-PAM) and $T=\log_2(L)/R_b$ is the symbol duration while $R_b$ is the bit rate of the incoming bit sequence $b_k$.

Direct detection is realized via a photodetector receiver which produces an output current, $r(t)$, proportional to the received instantaneous power. The received signal in the electrical domain is given by [2]:

$$r(t) = R \int_{-\infty}^{+\infty} x(\tau) h(t - \tau) d\tau + n(t) \tag{2}$$

where $h(t)$ is the channel's impulse response, $R$ the photodiode responsivity factor and $n(t)$ is a white Gaussian noise process, [10] with double-side PSD $N_0$ .

### A. Calculation of the impulse response

Several techniques have been proposed for characterizing the indoor optical wireless channel. Recursive algorithms, [11], require a large amount of computational effort to evaluate the impulse response in a regular sized room. In the present work, the modified Monte Carlo method [12] is used to evaluate $h(t)$. In this model, a number of rays, following a Lambertian radiation pattern, is generated at the transmitter site according to the method proposed in [13]. The line-of-sight component to the receiver is calculated by:

$$P_{LOS} = P_{tx} \frac{m+1}{2\pi} \frac{1}{D^2} A(\phi) \cos^m \theta \tag{3}$$

where $P_{tx}$ is the transmit power, $m$ is the mode number of the Lambertian source, $A(\phi)$ is the effective area of the receiver, $\theta$ is the angle between the ray and the normal to the transmitter's plane, $\phi$ is the angle between the ray and the normal to the receiver's plane, and $D$ is the distance between the emitter and the receiver, as depicted in Figure 2.

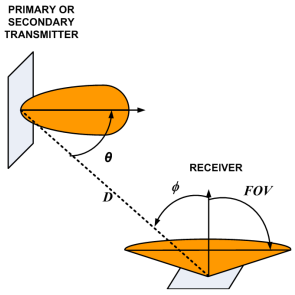


Figure 2.Definition of the angles $\theta$ and $\phi$.

The effective area of a receiver, using an optical concentrator [14], is given by:

$$A(\phi) = \frac{n^2 A_{\text{det}}}{\sin^2 \phi_c} \cos\phi \, \text{rect}(\phi, \phi_c) \tag{4}$$

where $A_{det}$ is the optical detector area, $n$ is the refractive index and $\phi_c$ the cut-off angle of the optical concentrator. Each ray generated, is reflected at the walls of the room and at each bounce, the LOS contribution is calculated according to (3) considering the reflectivity of the wall. The impulse response is obtained taking into account the amount of power reaching the receiver at a given time $t$. It should be noted that all rays produce as many LOS components as they suffer reflections, making this algorithm far more efficient than the conventional Monte Carlo method [13]. The ray-tracing algorithm described above was developed in MATLAB by the authors taking into account up to third order reflections.

### B. Ambient Light Noise

All surfaces in the room may act as ambient light sources. They are modeled as planar Lambertian transmitters with emissions based on measurement data [7]. Eight ceiling 100(W) tungsten floodlights are also assumed. Measurements of these lamps, [7], show that an accurate model for their radiant intensities is a generalized Lambertian pattern [9] of order $n_{\text{lamp}}$=2 with optical spectral density $p_{\text{lamp}}$=0.037 (W/nm). For data rates of the order 100Mb/s, the background-light induced shot noise is stationary with double-side PSD $S_{shot}=qA_{\text{det}}Ri_{bg}$, where $q$ is the electron charge, $R$ the receiver responsivity and $i_{bg}$ is the irradiance of the background light on the detector surface. The irradiance

$i_{bg}$ is calculated using an in-house tool developed in MATLAB according to:

$$i_{bg} = \Delta\lambda \sum_{C_i} \int_{C_i} S_i(\mathbf{r}_t) \frac{\cos\theta_i(\mathbf{r}_t,\mathbf{R})}{\pi D^2(\mathbf{r}_t,\mathbf{R})} \frac{A\left(\phi_i(\mathbf{r}_t,\mathbf{R})\right)}{A_{\text{det}}} d\mathbf{r}_t + \Delta\lambda\, p_{lamp} \frac{n_{lamp}+1}{2\pi} \sum_j \frac{\cos^{n_{lamp}}\theta_j(\boldsymbol{L}_j,\mathbf{R})}{D^2(\boldsymbol{L}_j,\mathbf{R})} \frac{A\left(\phi_j(\boldsymbol{L}_j,\mathbf{R})\right)}{A_{\text{det}}} \quad (5)$$

where $S_i(\mathbf{r}_t)$ is the spectral radiant emittance at the point $\mathbf{r}_t$ of surface $i$, $\theta_i$ is the angle between the normal of the emitter $i$ and the receiver-emitter line, $\phi_i$ is the angle between the normal of the detector and the emitter-detector line, $R$ is a 1×5 vector representing the position and orientation of the receiver [11], $L_j$ is another 1×5 vector representing the position and orientation of a lamp point noise source $j$, $D(\bullet)$ is the distance between receiver and source. Besides the background light noise, thermal noise at the receiver should be also taken into account. Considering a transimpedance preamplifier with a bipolar junction transistor in the first stage, the capacitance of the photodiode is $C_{\text{det}}=A_{\text{det}}c_{\text{src}}$, where $c_{\text{src}}=30\text{pF/cm}^2$, the double-side PSD of thermal noise in each receiver is modeled by [7]:

$$S_{thermal}(f) = \frac{2kT}{R_f} + qI_b + 2kT\left(2\pi f\right)^2 \times \left[ C_{\text{det}}^2 R_{base} + \left(C_{\text{det}} + C_\pi\right)^2 \left( \frac{1}{2g_m} + \frac{1}{R_c g_m^2} \right) \right] \quad (6)$$

where $R_{\text{f}}$ is the feedback resistor, $I_{\text{b}}$ is the front-end transistor base current, $g_{\text{m}}$ is the transistor transconductance and $C_\pi$ is the base-collector capacitance. The temperature, $T$, is in Kelvin, $q$ is the charge of an electron and $k$ denotes Boltzmann's constant. It is assumed that $I_b$=19.5μA, $R_f$=2.5kΩ, $C_\pi$=1.7pF, $R_{\text{c}}$=146Ω, $R_{base}$=68Ω and $g_m$=70mS.

As mentioned above, the detection is performed by a photodiode. The shot noise, in the photodiode, induced by the optical signal is $10^{-2}$ to $10^{-4}$ times smaller than that due to the background light [15], and thus it can be neglected.

### C. Signal Detection

In addition to noise, ISI is also an important degradation factor for indoor infrared wireless systems especially at high data rates. To mitigate the effects of ISI, several detection schemes have been proposed [6], [16]. In the case of the unequalized system, the SNR is given by:

$$SNR_U = \min_{(i,j)} \left\{ \left\langle \frac{\left(m_i - m_j\right)^2}{2N_0} \right\rangle \right\} \quad (7)$$

where $m_i$ is the received signal power when symbol $i$ is transmitted and $N_0=(S_{\text{shot}}+S_{\text{thermal}})*(1/T)$. In the presence of ISI, for a symbol transmitted at time $t_0$=0, one needs to calculate the values of $SNR_U$ considering the adjacent symbols at $\pm kT$, $k\neq 0$. The parameters $m_i$ are calculated using:

$$m_i = P_p \sum_k a_k \left( \frac{1}{T} \int_{-T/2}^{T/2} p(\tau - kT) d\tau \right) \quad (8)$$

and assuming that the values of the symbol sequence $a_k$ are such that the symbol transmitted at $t_0$=0 corresponds to $i$. In (8), $p(t)$ is a rectangular pulse $rect(t)$ (height=1 and width=$T$) passed through a baseband filter which represents the combined effects of the transmitter shaping, $g_{\text{tx}}(t)$, the infrared channel propagation, $h(t)$, and the photodiode responsivity. The values obtained by (8) are averaged with respect to the adjacent symbols at $\pm kT$, $k\neq 0$.

The performance of the MLSE cannot exceed the Matched Filter Bound (MFB) given by [17], [18]:

$$SNR_{MFB} = \frac{P_p}{N_0} \int_{-\infty}^{+\infty} M(f) df \quad (9)$$

where

$$M(f) = \frac{1}{S_n(f)} \left| \int_{-\infty}^{+\infty} p(t) e^{j2\pi ft} \right|^2 \quad (10)$$

In (9), $M(f)$ is the frequency spectrum of the matched filter's output pulse. In practice, the MLSE may be complex to implement leading to an excessive processing delay which is inappropriate for wireless applications. Alternatively, LE or DFE equalization schemes are suboptimal strategies for detecting signals in the presence of ISI, their primary advantage being a reduction in complexity. For the LE equalizer, the SNR is given by [17], [18]:

$$SNR_{LE} = \frac{P_p}{N_0} \left( \int_{-1/2T}^{1/2T} \frac{df}{S(f)} \right)^{-1} \quad (11)$$

while for the DFE, the SNR becomes:

$$SNR_{DFE} = \frac{P_p T}{N_0} \exp\left( T \int_{-1/2T}^{1/2T} \ln\left[S(f)\right] df \right) \quad (12)$$

The spectrum $S(f)$ is given by:

$$S(f) = \frac{N_0}{P_p T} + \frac{1}{T^2} \sum_k M\left( f + \frac{k}{T} \right) \quad (13)$$

## III. Results and Discussion

In order to evaluate the effect of different transmitter-receiver configurations on the performance of a wireless infrared link, a number of simulations were performed for the medium-sized office room, depicted in the inset of Figure 3. Table I, outlines the basic configuration parameters for the simulation. In the table, $\rho_{\text{north}}$, $\rho_{\text{south}}$, $\rho_{\text{east}}$, $\rho_{\text{window}}$, $\rho_{\text{ceiling}}$ and $\rho_{\text{floor}}$ denote the reflectivities of the corresponding surfaces of the room, $L_{\text{x}}$, $L_{\text{y}}$ and $L_{\text{z}}$ are the room dimensions along the $x$, $y$ and $z$ axis respectively, depicted in the inset of Figure 3. HPSA is the Half Power Semi Angle of the transmitter, which is related to the order $m$ of the transmitter radiation pattern through $m$=-ln2/ln(cos(HPSA)).

Table I
Configuration Parameters

| *PARAMETERS* | *T1R1* | *T8R8* |
|---|---|---|
| **Room** | | |
| $(L_x,L_y,L_z)$ | (5.5,7.5,3.5) | (5.5,7.5,3.5) |
| $\rho_{east}$ | 0.3 | 0.3 |
| $\rho_{south}$ | 0.56 | 0.56 |
| $\rho_{north}$ | 0.3 | 0.3 |
| $\rho_{window}$ | 0.04 | 0.04 |
| $\rho_{ceiling}$ | 0.69 | 0.69 |
| $\rho_{floor}$ | 0.09 | 0.09 |
| **Transmitter** | | |
| HPSA | 1x60° | 6 x 30°+2 x 30° |
| Azimuthal separation | 0 | 6 x 45° |
| elevation | 1 x 90° | 6 x 0°+2 x 90° |
| position | (2,4,1.5) | (2,4,1.5) |
| **Receiver** | | |
| FOV(φc) | 60° | 31° |
| Position | NW-SE diagonal height: 0.8m | NW-SE diagonal height: 0.8 |

For the T1R1 configuration [7], the transmitter has a first order Lambertian pattern and is oriented vertically towards the ceiling. The receiver is a pin photodetector of area $A_{det}$=1cm$^2$ with an optical concentrator having cutoff angle of 60$^0$ and refractive index $n_c$=1.44, while the optical filter has a bandwidth $\Delta\lambda$=50nm. For the T8R8 configuration [7] the transmitter uses six equal power 30$^0$ HPSA transmit beams equally spaced in the horizontal plane and two such identical beams pointing straight up. The receiver uses eight optical concentrators with cut-off angles 31$^0$, seven of which are horizontally oriented and one is pointing straight up. The power collected from each receiver is added together to obtain the total received power.

The transmit power equals 0.6W and the bit-rate of the system under examination is 100 Mbps. The transmitter has a center wavelength of 806nm and is located at a height of 1.5 m, near the center of the room. The SNR at different positions of the receiver along the south-east north-west diagonal of the room was calculated.

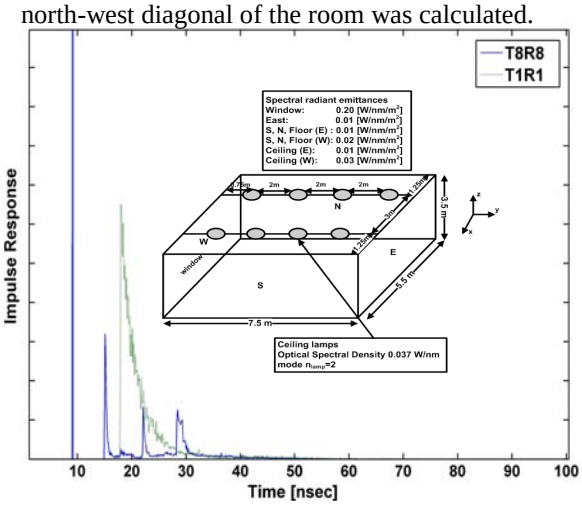


Figure 3. Impulse response of the optical wireless channel for configurations T8R8 and T1R1.

The electrical SNR for the vertical configuration, T1R1, is depicted in Figures 4, 5 and 6, for OOK, 4-PPM and 4-PAM respectively, when different equalization schemes are employed. In Figure 4 one can observe that, in the case of OOK modulation the maximum achievable SNR is 19dB at the center of the room when no equalization is used, whereas a large drop of almost 14dB can be observed in the corners of the room. The use of equalization schemes can improve the performance of the system by 5 to 7 dB in the case of DFE and MLSE receivers respectively.

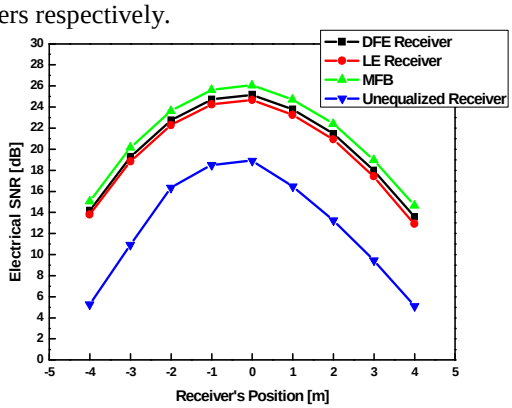


Figure 4.SNR for OOK modulation for the T1R1 configuration.

When 4-PPM is used, **Figure 5**, the maximum SNR that can be achieved according to the MFB is 28 dB in the center of the room, whereas near the corners it does not drop below 16dB. The DFE and LE schemes perform almost equally well, achieving an SNR of 26 dB and 25 dB respectively.

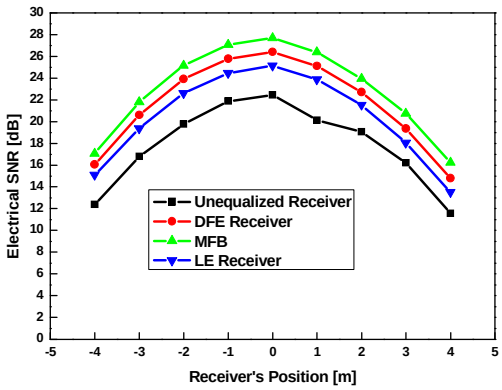


Figure 5. SNR for 4-PPM modulation for the T1R1 configuration.

Figure 6 illustrates the electrical SNR when 4-PAM is employed. According to the MFB curve, the SNR cannot exceed the value of 30 dB at the center of the room whereas near the corners it does not drop below 20 dB. The DFE and LE schemes improve the performance of the unequalized system by almost 9 and 8 dB respectively.

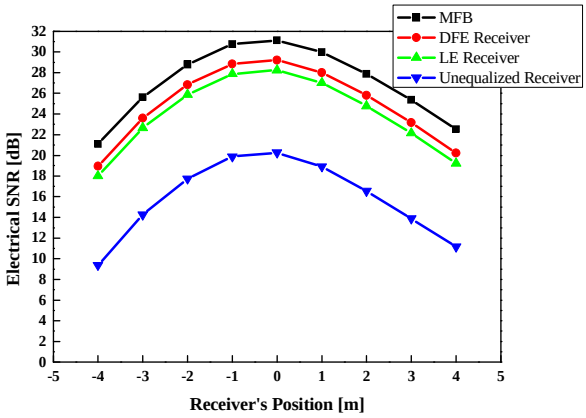


Figure 6. SNR for 4-PAM modulation for the T1R1 configuration.

By comparing Figures 4, 5 and 6, it can be observed that the PPM and PAM schemes outperform OOK even in the unequalized receiver's case. More specifically, when no equalization method is employed, PPM exhibits the best behavior. When DFE and LE are employed in combination to a PAM scheme, even for the worst-case SNR at the corners of the room, a first estimation of the Bit Error Rate (BER), assuming Gaussian statistics, would be less than $10^{-6}$. Hence the system can provide a reliable and robust link for a bit rate of 100 Mbps.

Considering the location of the receiver for the lowest SNR at 100Mb/s, the values for the SNR obtained for higher bit rates, up to 200 Mbps were estimated and are depicted in Figure **7**, 8 and 9. From these diagrams it is deduced that for the OOK equalized schemes, 90Mb/s is the maximum bit rate that can be supported, if SNR values higher than 14dB are required. On the other hand, 4-PPM and 4-PAM can support up to 110Mb/s and 120 Mb/s respectively even at such unfavorable positions in the room.

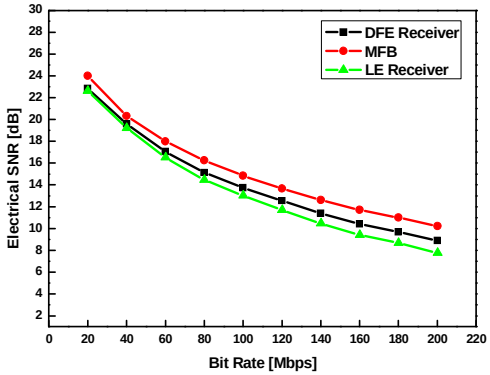


Figure 7. Worst case SNR for OOK modulation for the T1R1 configuration for various bit rates.

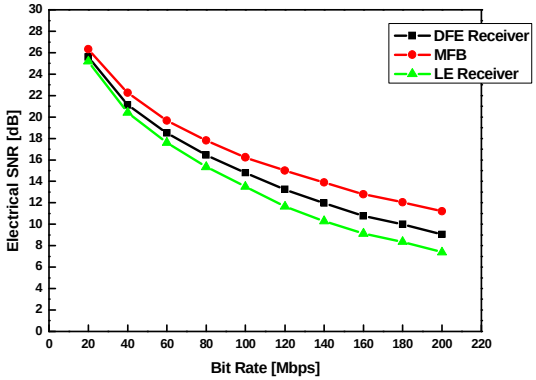


Figure 8. Worst case SNR for PPM modulation for the T1R1 configuration for various bit rates.

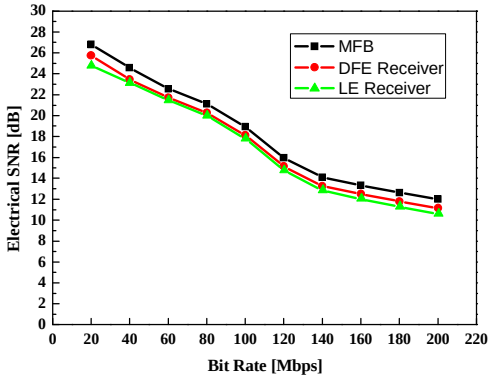


Figure 9. Worst case SNR for PAM modulation for the T1R1 configuration for various bit rates.

Better coverage can be obtained using the T8R8 transmitter/receiver configuration. The values of the SNR obtained at different receiver positions, are depicted in Figure **10**, 11 and 12. Comparing these values with the ones in Figures 4, 5 and 6 it is deduced that there are no large variations in the values of the SNR and hence, the system performance is not expected to vary significantly (except at the edges of the room). As in the case of T1R1, PAM generally outperforms OOK and PPM, and both the LE and DFE equalization techniques significantly improve the system performance. For example, if one excludes the SNR values obtained at receiver positions near the two edges of the diagonal, the SNR for T8R8-4-PAM is higher than 20dB implying a BER much less than $10^{-14}$. The worst case SNR is again obtained at the edge of the room and for the case of the equalized schemes is approximately the same as those obtained by T1R1. The variations in the SNR values at different positions along the main diagonal of the room can be interpreted in combination to the impulse response obtained for both configurations, see

Figure 3. It is deduced that in the T8R8 impulse response four peaks are observed while in the T1R1 only one. This can be attributed to the horizontal transmit and receive lobes of the T8R8 configuration and it is the reason for the different shapes of the SNR distribution between T8R8 and T1R1. These results seem to indicate that the T8R8-4-PAM and T8R8-4-PPM configurations can carry ≥100Mb/s (Fast Ethernet type) data rates in almost every

point in the room and should be considered favorably as a potential hot spot for future indoor WLANs.

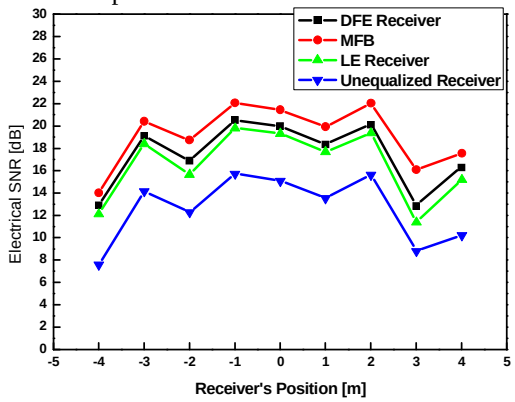


Figure 10. SNR for OOK modulation for the T8R8 configuration.

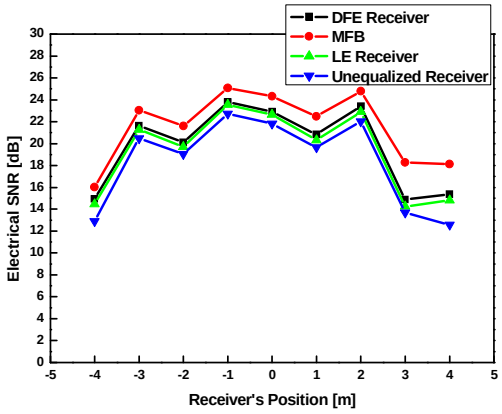


Figure 11. SNR for 4-PPM modulation for the T8R8 configuration.

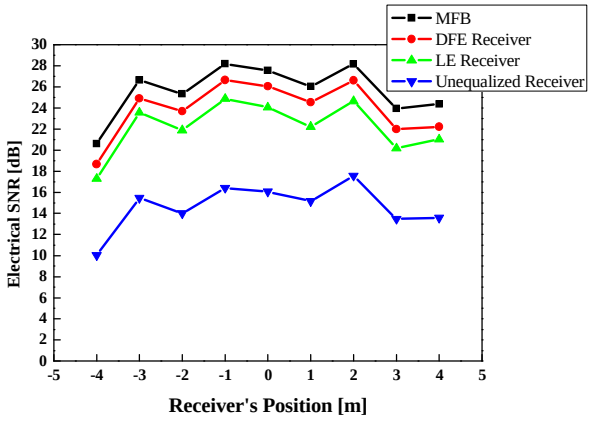


Figure 12. SNR for 4-PAM modulation for the T8R8 configuration.

## IV. CONCLUSIONS

In this paper, the potential of indoor optical wireless systems based on non-directed configuration was examined for data rates of 100Mb/s and beyond. It was shown that with the use of suitable equalization schemes (DFE or LE) and modulation formats such as the 4-PPM and 4-PAM, it is possible to reliably carry traffic of 100Mb/s inside a medium size room. Given the robust nature of these configurations, non-directed systems could provide an attractive candidate for future, high speed WLANs.

## ACKNOWLEDGMENT

The research leading to these results has received partial funding from the European Community's Seventh Framework Program FP7/2007-2013 under grant agreement n° 213311 also referred as OMEGA.

## REFERENCES

[1] F.R. Gfeller and U. Bapst, "Wireless in-house data communication via diffuse infrared radiation," *Proc. IEEE*, vol. 67, pp. 529–551, November 1979.

[2] J.M. Kahn, W.J. Krause and J.B. Carruthers, "Experimental characteristization of non-directed indoor infrared channels," *IEEE Trans. On Comm.*, vol. 43, pp. 1613–1623, April 1995.

[3] A.C. Boucouvals, "Indoor ambient light noise and its effect on wireless optical links," Proc. *Optoelectronics IEE*, vol. 143, pp. 334–338, December 1996.

[4] A. J.C. Moreira, R.T. Valadas, and A.M. de Oliveira Duarte, "Characteristization and modeling of artificial light interference in optical wireless communication systems," *Proc. IEEE Personal Indoor and Mobile Radio Communications (PIMRC '95)*, vol. 1, pp. 326–331, September 1995.

[5] A. J.C. Moreira, R.T. Valadas, and A.M. de Oliveira Duarte, "Optical interference produced by artificial light," *Wireless Networks.*, vol. 3, pp. 131–140, May 1997.

[6] G.W. Marsh and J.M. Kahn, "50-Mb/s diffuse infrared free-space link using on-off keying with decision feedback," *IEEE Photonics Technology Letters*, vol. 6, pp. 1268–1270, October 1994.

[7] J.B. Carruthers and J.M. Kahn, "Angle diversity for non-directed wireless infrared communication," *IEEE Trans. On Comm.*, vol. 48, pp. 960–969, June 2000.

[8] G.Ntogari, T. Kamalakis and T. Sphicopoulos, "Performance analysis of non-directed equalized indoor optical wireless systems," Proc. IEEE CSNDSP 08, pg 156-160, July 2008.

[9] J.M. Kahn and J.R. Barry, "Wireless infrared communications," *Proc. IEEE*, vol. 85, pp. 265–298, February 1997.

[10] M.D. Audeh, J.M. Kahn, and J.R. Barry, "Performance of PPM with maximum-likelihood sequence detection on measured non-directed infrared channels," *IEEE Proc. Inter. Conf. on Comm.*, vol.2, pp. 1177-1181, June 1995.

[11] J.R. Barry, J.M. Kahn, W.J. Krause, E.A. Lee, and D.G. Messerschmitt, "Simulation of multipath impulse response for indoor wireless optical channels," *IEEE Journal on Selected Areas in Communications*, vol. 11, pp. 367–379, April 1993.

[12] F.J. Lopez-Hernandez, R. Perez-Jimenez, and A. Santamaria, "Modified Monte Carlo scheme for high-efficiency simulation of the impulse response on diffuse IR wireless indoor channels," *Electronics Letters*, vol. 34, pp. 1819–1820, September 1998.

[13] F.J. Lopez-Hernandez, R. Perez-Jimenez, and A. Santamaria, "Monte Carlo calculation of impulse response on diffuse IR wireless channels," *Electronics Letters*, vol. 34, pp. 1260–1262, April 1993.

[14] W. Welford and R. Winston, *High Collection Nonimaging Optics*, New York: Academic, 1989.

[15] R.M. Gagliardi and S.Karp, *Optical Communications*, John Wiley & Sons, New York, NY 1976.

[16] D.C.M. Lee and J.M. Kahn, "Coding and equalization for PPM on wireless infrared channels," *IEEE Trans. On Comm.*, vol.47, pp. 500-503, February 1999.

[17] Q. Yu and A. Shanbhag, "Electronic data processing for error and dispersion compensation," *Journal of LIghtwave Technology*, vol.24, pp. 4514-4525, December 2006.

[18] J.G. Proakis, *Digital Communication*, 4th ed., New York: Mc Graw-Hill, 1995, pp. 601-626.

**Georgia Ntogari** was born in 1980. She received her Diploma in Electrical and Computer Engineering from the Aristotle University of Thessaloniki in 2004 and MSc in Communications Engineering from the Technical University of Aachen, Germany, in 2006. She is currently a PhD student in the Department of Informatics and Telecommunications at the National University of Athens. Her research interests include indoor optical wireless communication systems.

**Thomas Kamalakis** was born in 1975 and obtained his BSc in Informatics and MSc in Telecommunication with distinction, from the University of Athens in 1997 and 1999 respectively. In 2004 he completed his PhD thesis in the design and modeling of Arrayed Waveguide Grating devices in the same institution. Since 2008 he is a Lecturer in the Department of Informatics and Telematics in the Harokopio University of Athens. His research interests include photonic crystal and optical wireless devices as well as non-linear effects in optical fibers.

**Thomas Sphicopoulos** received the Physics degree from Athens University in 1976, the D.E.A. degree and Doctorate in Electronics both from the University of Paris VI in 1977 and 1980 respectively, the Doctorat Es Science from the Ecole Polytechnique Federale de Lausanne in 1986. From 1976 to 1977 he worked in Thomson CSF Central Research Laboratories on Microwave Oscillators. From 1977 to 1980 he was an Associate Researcher in Thomson CSF Aeronautics Infrastructure Division. In 1980 he joined the Electromagnetism Laboratory of the Ecole Polytechnique Federal de Lausanne where he carried out research on Applied Electromagnetism. Since 1987 he is with the Athens University engaged in research on Broadband Communications Systems. In 1990 he was elected as an Assistant Professor of Communications in the Department of Informatics & Telecommunications, in 1993 as Associate Professor and since 1998 he is a Professor in the same Department. His main scientific interests are Microwave and Optical Communication Systems and Networks and Techno-economics. He has lead about 40 National and European R&D projects. He has more than 100 publications in scientific journals and conference proceedings. From 1999 he is advisor in several organizations including EETT (Greek NRA for telecommunications) in the fields of market liberalization, spectrum management techniques and technology convergence.